JACS
JOURNAL OF THE AMERICAN CHEMICAL SOCIETY

Communication

pubs.acs.org/JACS

Dynamically Interchangeable Nanoparticle Superlattices Through the Use of Nucleic Acid-Based Allosteric Effectors

Youngeun Kim,[†,§] Robert J. Macfarlane,[‡,§] and Chad A. Mirkin*[,†,‡,§]

[†]Department of Materials Science and Engineering, [‡]Department of Chemistry, and [§]International Institute for Nanotechnology, Northwestern University, 2145 Sheridan Road, Evanston, Illinois 60208-3113, United States

Supporting Information

ABSTRACT: DNA is a powerful tool for programmably assembling colloidal crystals, and has been used to generate nanoparticle superlattices with synthetically adjustable lattice parameters and crystal symmetries. However, the majority of these superlattice structures remain static once constructed, and factors such as interparticle distance cannot be controlled in a facile and rapid manner. Incorporation of these materials into functional devices would be greatly benefitted by the ability to change various aspects of the crystal assembly after the lattice has been synthesized. Herein, we present a reversible, rapid, and stoichiometric on-the-fly manipulation of nanoparticle superlattices with allosteric effectors based upon DNA. This approach is applicable to multiple different crystal symmetries, including FCC, BCC, CsCl, and AlB_2.

When nanoparticles are coated with a dense monolayer of DNA, they become programmable atom equivalents (PAEs) that can be used for the construction of a wide variety of functional materials.[1−3] These PAEs, which already form the basis for FDA-cleared medical diagnostic tools,[4−6] intracellular probes,[7−10] and new therapeutic candidates,[11,12] can then be assembled into superlattices just as naturally occurring atoms are assembled into solid state structures.[13−20] However, unlike atoms, these PAEs allow one to control the crystal lattice symmetry and lattice parameters independent of the nanoparticle core identity. The formation, structure, and emergent properties of PAE superlattices have been studied extensively,[21−24] leading to a set of design rules that allow for a priori predictions of crystal stability and unique optical phenomena.[3,17] One of the unusual features of lattices formed in this manner is the dynamic character of the DNA "bonds" that hold the structure together. In principle, one could have dynamically interchangeable lattices through the proper design of DNA interconnects. Attempts in this direction have been made, but with limited success. One structure has been reported based upon single strands with deliberately designed hairpins.[25] These structures allow one to increase the lattice constant by reacting a pre-formed lattice with an entity that opens or closes the hairpin but not in a reversible manner. Indeed, the structures do not show the ability to re-attain their starting states, and the time required for the interconversion is on the hour time scale. Herein, we describe a new duplex design with a hairpin structure that can be driven to the opened and closed states in such a way that the crystal symmetry is maintained and the lattice parameter cleanly changes over the 3−12 nm range, back and forth through multiple cycles over a time scale of seconds (Figure 1). This process can be implemented with sub-nm precision, emphasizing the importance of the duplex design and providing access to the first DNA-programmable assemblies where lattice structure can be dynamically interconverted on the fly.

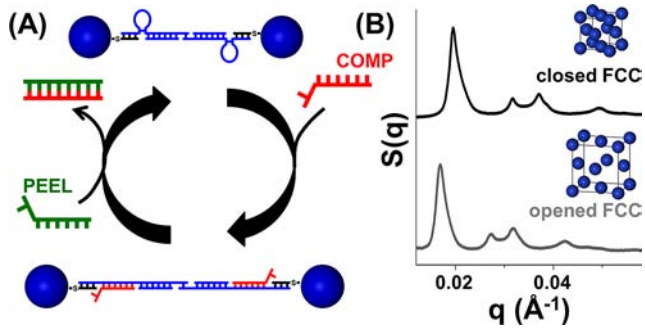

Figure 1. (A) Simplified scheme of the opening and closing of stem−loop structures and changing the interparticle distance. "Comp" strand shown in red; "peel" strand displayed in green. The addition of "comp" strands opens the stem−loop structures and therefore increases the lattice constant. Addition of "peel" strands closes the stem−loops, decreasing the lattice constant, and returning the lattice to its initial, closed state. (B) SAXS patterns of PAE superlattices with an FCC crystal structure in both opened and closed states. The lattice constant at the opened state is greater, indicated by the principle peak's location at a lower q value.

PAE superlattices are constructed by first functionalizing gold nanoparticles with DNA that include terminal alkylthiol moieties; the strong gold−surface bonds enable a dense monolayer of oriented oligonucleotides to form on the particle surfaces.[1,17] Then, linker DNA strands are added that hybridize to the surface-bound DNA, where each linker strand is composed of three segments: (1) a recognition sequence that is complementary to the thiolated DNA, (2) a spacer sequence to controllably adjust the desired DNA length, and (3) a sticky-end sequence that facilitates assembly of PAEs by allowing the linkers on particles to hybridize to each other (Figure 1).[17,18] Two PAEs will form DNA linkages only if they contain complementary sticky-ends, thereby allowing for control over

Received: June 14, 2013
Published: July 3, 2013

   dx.doi.org/10.1021/ja405988r | J. Am. Chem. Soc. 2013, 135, 10342−10345

the bonding interactions between nanoparticles. In this work, stem−loop structures were placed in the spacer region to easily vary the overall length of the linker strands.

A stem−loop, also known as a DNA hairpin, is an intramolecular base-pairing configuration that occurs in a single-stranded oligonucleotide. This structure includes two regions: (1) a stem portion consisting of two complementary sequences that can form a duplex with each other and flank the second region, (2) a loop portion with un-paired bases that is typically 4−8 bases long. One can use such stem−loop DNA to interchangeably access an "extended" and a "contracted" state by adding or removing a strand that is fully complementary to both the stem and loop regions, thereby resulting in a change in the overall length of the DNA (Figure 1).[26,27] Consequently, stem−loop DNAs can act as small molecule allosteric effectors to manipulate larger scale PAE superlattices. If a DNA linkage between two particles contains a stem−loop structure, the change in overall length of the stem−loop DNA can translate into a shift in interparticle distance, and therefore alter the lattice constant of the PAE superlattices.

To incorporate stem−loops into a superlattice structure, 67-mer linker DNA strands were synthesized containing a 20-base stem−loop structure within its sequence. This design allowed the 67-base linkers to access two states: (1) a contracted, or closed, state where the stem−loop structure forms a short, internal loop, and (2) an extended, or opened, state where the stem−loop structure is duplexed with a second strand that contains a sequence complementary to the stem−loop sequence. When 27-mer oligonucleotides complementary to the stem−loop ("comp" strands, red in Figure 1) were introduced to the linker strands on the PAEs, the "comp" strands form duplexes with the stem−loop structures over a 20 base region. The additional seven bases in the 27-mer "comp" strand acted as a toehold, providing extra bases to facilitate the transition from the opened to the closed state.[28] After the stem−loop structure became fully duplexed in its opened state, another set of 27-mer oligonucleotides ("peel" strands, green in Figure 1) were added to the system. These "peel" strands were fully complementary to the "comp" strands over all 27 bases, including the toehold. Because it is more thermodynamically favorable for the "comp" strands to hybridize with the "peel" strands due to the seven additional base pairings from the toehold sections of the oligonucleotides, the "comp" strand is removed from the lattice, resulting in the formation of the original stem−loop structure and a return to the initial lattice constant.

PAE superlattices were first constructed with stem−loop structures on their linker strands to confirm that the steric bulk of the stem−loop structure did not inhibit the formation of colloidal crystals. Specifically, PAE superlattices were assembled into a face-centered cubic (FCC) crystal structure, in which all PAEs had self-complementary sticky-ends. Two different designs of the 67-base linker strands were tested: one where the stem−loop was placed near the sticky-end (1 base away) and the other where the stem−loop was placed far from the sticky-end (10−20 bases away) and closer to the particle (for sequences, see Supporting Information (SI)). When the stem−loop structure was located near the sticky-end, aggregation did not occur. We hypothesize that the bulkiness of the stem−loop structures near the sticky-ends provided a steric hindrance that prevented the sticky-ends from coming together. Thus, PAEs were not able to interact and aggregate because the sticky-ends could not bind to each other. On the other hand, when the stem−loop was placed 10−20 bases away from the sticky-end, the PAEs assembled and precipitated from solution. These aggregates were then annealed just below their melting temperature to form crystalline superlattices. It is important to note that, although the stem−loop structures were predicted to have a lower melting temperature than fully duplexed DNA strands of equivalent length,[29] the annealing process necessary to form crystalline structures did not melt apart the stem−loop structures. This was confirmed by assembling two different sets of superlattices—one in which the stem−loop structure was intact, and another where the stem−loop linker had been duplexed to a "comp" strand prior to adding the linkers to the nanoparticles. These two sets of PAE superlattices in the closed and opened states were then characterized via in situ small-angle X-ray scattering (SAXS) to determine their crystal symmetry and lattice constant. SAXS data confirmed the PAEs had adopted an FCC crystal structure with a ∼10 nm difference in lattice constants between opened (65 nm) and closed (55 nm) states. This result supported our hypotheses that incorporating stem−loop structures in DNA linkers enables PAEs to access two different lattice constants of PAE superlattices, and the presence of the stem−loop did not interfere with the crystallization process.

These PAE superlattices were then tested to determine if they could be toggled between the two different stem−loop states, even within the assembled lattice structure. Figure 2 shows the SAXS results of dynamically toggling between the opened and closed states of PAE superlattices with a FCC crystal symmetry. PAE superlattices were first assembled with the stem−loops in the closed state. Then, "comp" strands were added in a 1:1 ratio to the 67-base linkers to open the stem−loop structure into a fully hybridized duplex. SAXS confirmed a transition from the closed to the opened state as the peak position shifted to lower values upon introduction of the "comp" strand, indicating an increase in the interparticle distance and lattice constant. Next, an equal number of peel strands was added to the comp strands to close the stem−loop structure. A return of the linkers to their original closed state was noted by the scattering peak positions returning to their initial values, indicating a decrease in the interparticle distance

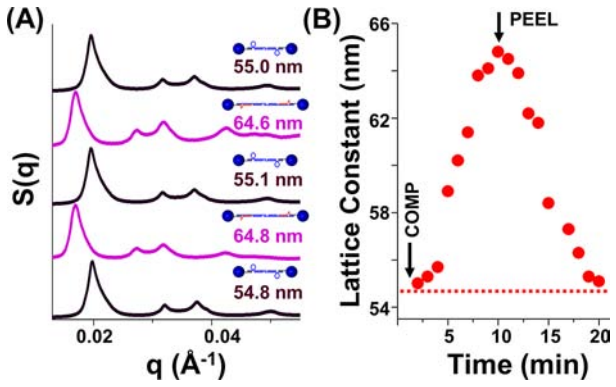

Figure 2. (A) Reversibility of opening and closing of PAE superlattices with FCC structure. Two cycles of opening and closing are shown from bottom to top, and lattice parameters are noted for each SAXS scan. (B) Rate of the opening and closing of an FCC superlattice. Full opening and complete closing occur in 8−10 min after addition of "comp" or "peel" strands, respectively. The initial lattice constant at a closed state is denoted as a dotted line. (Note that with vigorous stirring, the transition occurred in less than 2 min.)

and reversion of the lattice to its initial lattice constant. It is important to note that both of the changes were done with stoichiometric amounts of the "comp" and "peel" strands, and that the starting and final lattice parameters were within 1% of each other, indicating complete reversibility.

By subsequent additions of "comp" and "peel" strands, we were able to cleanly cycle through multiple openings and closings of the stem–loop structure, and consequently expand and contract the PAE superlattices, respectively. "Comp" and "peel" strands were consecutively added to FCC PAE superlattices to transition the system between the two states until the sample disintegrated due to extended X-ray beam exposure. Across all cycles, the transitions showed complete reversibility with the lattice constants of the opened and closed states varying by as little as 0.2 nm (0.4%).

For the one other system that utilized stem–loops to effect lattice parameter changes studied in the literature, the switch between opened and closed states took several hours for the transition to occur and required excess oligonucleotide, heat, and multiple washing steps. In comparison, this system undergoes a change between the binary states simply through the addition of stoichiometric amounts of the allosteric oligonucleotide effectors in less than 2 min at room temperature. Significantly, when the comp or peel strands were allowed to diffuse without stirring, the change in lattice constant occurred within 8–10 min, indicating that the diffusion of DNA was the rate limiting step in effecting the transition (Figure 2).

We further demonstrated that this allosteric effector approach to reversibly expand and contract a lattice could also be applied to more complex crystal structures such as body-centered cubic (BCC), CsCl, and AlB_2, all of which can be made via literature-based design rules (Figure 3). Each of

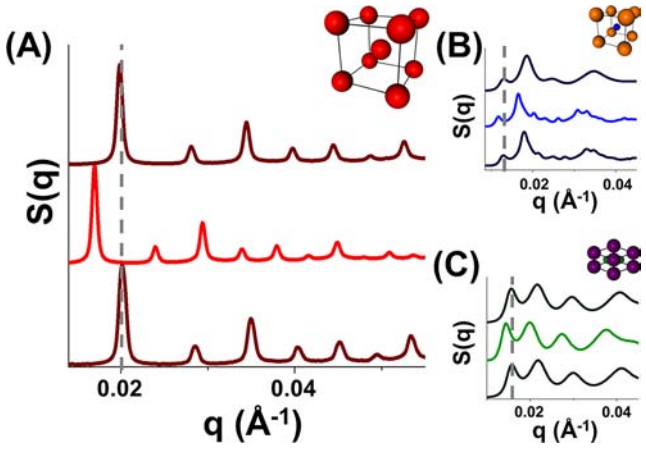

Figure 3. Opening and closing of PAE superlattices in (A) BCC, (B) CsCl, and (C) AlB_2 crystal structures.

these structures were synthesized with linkers that contained a stem–loop design similar to the design used in the FCC lattices (see SI), and each could be toggled between open and closed crystalline states, demonstrating the generality of this approach (see Table S2 for interparticle distances in the opened and the closed states).

In the systems described thus far, all stem–loops within a lattice contained identical stem–loop structures. However, in the binary (BCC, CsCl, AlB_2) systems, which utilize two batches of particles that have different unique linker strands, one can use two different nucleic acid effectors to sequentially address the stem–loop structures and effect discrete changes in lattice constant. For example, two different stem–loop sequences (67-bases) were loaded onto two separate batches of particles designed to form a BCC lattice. Using two different "comp" strands ("comp1", "comp2") and "peel" strands ("peel1", "peel2"), the PAE superlattices were transformed in a four-step manner starting from a closed system with a lattice constant of 42.2 nm (Figure 4). The addition of "comp1"

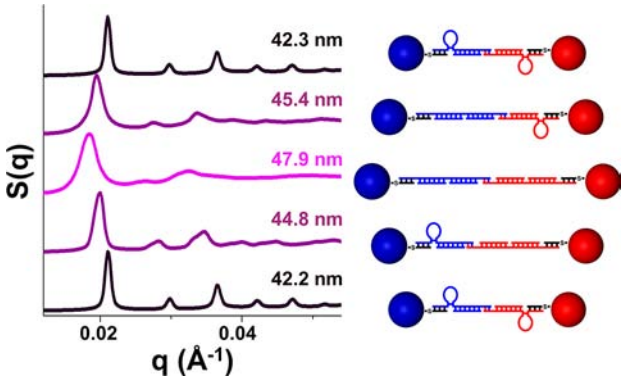

Figure 4. Orthogonally opening and closing of PAE superlattices to access intermediate crystalline states (transition from bottom to top).

strands opens up one set of particles, effectively increasing their hydrodynamic radii (44.8 nm) without disassembling the superlattice. Next, "comp2" strands were added to open up the other group of particles, expanding the PAE superlattices to the maximum extent (47.9 nm). To reverse the process, "peel1" strands were added to remove the comp1 strands and contract the lattice and re-form the intermediate structure (45.4 nm). To complete the cycle, "peel2" strands were added to return all possible stem–loop structures to their original states and return the superlattice to its initial closed state (42.3 nm). Again, each step was completely reversible, as the two interim states varied in lattice parameter by only 0.6 nm (44.8 and 45.4 nm), and the two closed states varied by only 0.1 nm (42.2 and 42.3 nm).

Finally, by including more than one stem–loop structure in each linker strand, the change in lattice constant could be varied between 3 and 12 nm. A 109-base linker strand was designed with two dissimilar 20-base stem–loop structures within its sequence (see SI). Both stem–loop structures were 20 bases apart and contained different base sequences to avoid complementary overlap with each other. One set of particles with these long linkers was combined with another set of particles with the initially designed 67-base linker strands (containing a single stem–loop). These PAEs formed superlattices with a BCC crystal symmetry. When all three separate stem–loop structures were opened up, the difference in lattice constants between the fully opened and closed states of the PAE superlattices was ~12 nm (Figure S1).

In summary, we have developed a method for using stem–loop structures and short strands of DNA to orthogonally and allosterically access different crystalline states of PAE assemblies, where the lattice parameters within such structures can be changed without disassembling the original lattice. The approach provides independent addressability of stem–loop structures and allows the lattices to be opened and closed in a cyclical manner via a diffusion-limited process. This ability to dynamically interconvert lattices made of PAEs likely will

dx.doi.org/10.1021/ja405988r | J. Am. Chem. Soc. 2013, 135, 10342–10345

become important in modulating the plasmonic, catalytic, and mechanical properties of this emerging class of materials.

■ ASSOCIATED CONTENT

Supporting Information

Experimental details and additional data. This material is available free of charge via the Internet at http://pubs.acs.org.

■ AUTHOR INFORMATION

Corresponding Author

chadnano@northwestern.edu

Notes

The authors declare no competing financial interest.

■ ACKNOWLEDGMENTS

This material is based upon work supported by the AFOSR through Award No. FA9550-11-1-0275 and the Northwestern University Non-equilibrium Energy Research Center (NERC), an Energy Frontier Research Center funded by the U.S. Department of Energy, Office of Science, Office of Basic Energy Sciences under Award Number DE-SC0000989. Additionally, C.A.M. is grateful for a NSSEFF Fellowship from the DoD.

■ REFERENCES

(1) Mirkin, C. A.; Letsinger, R. L.; Mucic, R. C.; Storhoff, J. J. *Nature* **1996**, *382*, 607.
(2) Cutler, J. I.; Auyeung, E.; Mirkin, C. A. *J. Am. Chem. Soc.* **2012**, *134*, 1376.
(3) Macfarlane, R. J.; O'Brien, M. N.; Petrosko, S. H.; Mirkin, C. A. *Angew. Chem., Int. Ed.* **2013**, *52*, 5688.
(4) Elghanian, R.; Storhoff, J. J.; Mucic, R. C.; Letsinger, R. L.; Mirkin, C. A. *Science* **1997**, *277*, 1078.
(5) Drummond, T. G.; Hill, M. G.; Barton, J. K. *Nat. Biotechnol.* **2003**, *21*, 1192.
(6) Rosi, N. L.; Mirkin, C. A. *Chem. Rev.* **2005**, *105*, 1547.
(7) Maxwell, D. J.; Taylor, J. R.; Nie, S. M. *J. Am. Chem. Soc.* **2002**, *124*, 9606.
(8) Katz, E.; Willner, I. *Angew. Chem., Int. Ed.* **2004**, *43*, 6042.
(9) Seferos, D. S.; Giljohann, D. A.; Hill, H. D.; Prigodich, A. E.; Mirkin, C. A. *J. Am. Chem. Soc.* **2007**, *129*, 15477.
(10) Zheng, D.; Seferos, D. S.; Giljohann, D. A.; Patel, P. C.; Mirkin, C. A. *Nano Lett.* **2009**, *9*, 3258.
(11) Giljohann, D. A.; Seferos, D. S.; Daniel, W. L.; Massich, M. D.; Patel, P. C.; Mirkin, C. A. *Angew. Chem., Int. Ed.* **2010**, *49*, 3280.
(12) Wang, Z.; Liu, H.; Yang, S. H.; Wang, T.; Liu, C.; Cao, Y. C. *Proc. Natl. Acad. Sci. U.S.A.* **2012**, *109*, 12387.
(13) Park, S. Y.; Lytton-Jean, A. K. R.; Lee, B.; Weigand, S.; Schatz, G. C.; Mirkin, C. A. *Nature* **2008**, *451*, 553.
(14) Nykypanchuk, D.; Maye, M. M.; van der Lelie, D.; Gang, O. *Nature* **2008**, *451*, 549.
(15) Cheng, W.; Park, N.; Walter, M. T.; Hartman, M. R.; Luo, D. *Nat. Nanotechnol.* **2008**, *3*, 682.
(16) Cheng, W.; Hartman, M. R.; Smilgies, D.-M.; Long, R.; Campolongo, M. J.; Li, R.; Sekar, K.; Hui, C.-Y.; Luo, D. *Angew. Chem., Int. Ed.* **2010**, *49*, 380.
(17) Macfarlane, R. J.; Lee, B.; Jones, M. R.; Harris, N.; Schatz, G. C.; Mirkin, C. A. *Science* **2011**, *334*, 204.
(18) Macfarlane, R. J.; Jones, M. R.; Senesi, A. J.; Young, K. L.; Lee, B.; Wu, J.; Mirkin, C. A. *Angew. Chem., Int. Ed.* **2010**, *49*, 4589.
(19) Jones, M. R.; Macfarlane, R. J.; Lee, B.; Zhang, J. A.; Young, K. L.; Senesi, A. J.; Mirkin, C. A. *Nat. Mater.* **2010**, *9*, 913.
(20) Auyeung, E.; Cutler, J. I.; Macfarlane, R. J.; Jones, M. R.; Wu, J. S.; Liu, G.; Zhang, K.; Osberg, K. D.; Mirkin, C. A. *Nat. Nanotechnol.* **2012**, *7*, 24.
(21) Lazarides, A. A.; Schatz, G. C. *J. Phys. Chem. B* **2000**, *104*, 460.
(22) Sebba, D. S.; Mock, J. J.; Smith, D. R.; LaBean, T. H.; Lazarides, A. A. *Nano Lett.* **2008**, *8*, 1803.
(23) Xiong, H.; van der Lelie, D.; Gang, O. *Phys. Rev. Lett.* **2009**, *102*, 015504.
(24) Jones, M. R.; Osberg, K. D.; Macfarlane, R. J.; Langille, M. R.; Mirkin, C. A. *Chem. Rev.* **2011**, *111*, 3736.
(25) Maye, M. M.; Kumara, M. T.; Nykypanchuk, D.; Sherman, W. B.; Gang, O. *Nat. Nanotechnol.* **2010**, *5*, 116.
(26) Chen, J. I. L.; Chen, Y.; Ginger, D. S. *J. Am. Chem. Soc.* **2010**, *132*, 9600.
(27) Lermusiaux, L.; Sereda, A.; Portier, B.; Larquet, E.; Bidault, S. *ACS Nano* **2012**, *6*, 10992.
(28) Green, S. J.; Lubrich, D.; Turberfield, A. J. *Biophys. J.* **2006**, *91*, 2966.
(29) Vallone, P. M.; Paner, T. M.; Hilario, J.; Lane, M. J.; Faldasz, B. D.; Benight, A. S. *Biopolymers* **1999**, *50*, 425.